Dear Reviewer,

We thank you much for your effort reading our manuscript so carefully and for your valuable advices. We strongly believe that the suggested changes and additions improved the manuscript a lot. Please find below a point-by-point reply to all your recommendations (in blue).

[1] In section 3.3 (background decay), examine in detail how the type of shaped pulse affects the MNR if the recently published superior background correction method (kernel inclusion) is used. It is crucial to include this in this work.

We agree with the reviewer that the novel approach including the background into the Kernel is a very efficient and convincing approach. We have added a new section in the main text where we clarified why we think that the MNR as we used it is the most feasible parameter for optimising settings for DEER.

As stated by equation (10) the measured raw data does not only consist of the desired form factor but includes a background contribution emerging from intermolecular interactions. A common way to deal with this, is to fit the background according to equation (11) and divide the raw data by the fit to obtain the form factor that can then be transformed into a distance distribution (Jeschke, 2012; Jeschke et al., 2006). When measuring DEER traces, a precise distance determination is desired. Since for an experimental parameter optimisation, the true underlying distance distribution is unknown, a metric is needed that is based on the recorded data. The MNR of the form factor is a suitable for this case as it increases with an increasing modulation depth and an increasing echo intensity. As the noise of the form factor increases towards its end due to the division by the background, the MNR goes down with a stronger background decay. It can therefore capture the fact that a larger background decay leads to less reliable distance distributions as has recently be investigated by [Fabregas, et. Al., 2020] in a detailed study. In their paper they also suggest a different method for background correction that treats the background by directly including it in the kernel that is needed to calculate the distance distribution from the DEER trace. As this methods renders the calculation of a form factor redundant, a MNR cannot be directly obtained by it. Even though this new method has shown itself to give more reliable distance distributions in the case of large background decays its performance still drops with an increasing background. Therefore, we consider the MNR that is obtained by the background correction by division still as the best measure to optimise settings for a DEER measurements experimentally.

We have also added a chapter in the SI to discuss the suitability of the MNR as a merit function if the background correction by kernel inclusion is used:

S2 The MNR as the function of merit

Here, we want to discuss whether the MNR is a suitable function of merit for the determination of distance distributions and up to which time point in the DEER trace, the MNR needs to be evaluated to serve this purpose. Therefore, we performed

simulations with a model distance distribution p_0 that is based on the narrow distance distribution of the model system used in this study. We approximated the experimentally obtained distance distribution with a Gaussian with a mean at 5.08 nm and a standard deviation of 0.08 nm. We varied the background density in ten steps from k = 0.01 1/µs to k = 0.3 1/µs in combination with a low, medium and high noise level (noise σ_0 = 0.02, 0.05 and 0.1) that was added to the DEER trace. The background dimension was set to d = 3 and a modulation depth of 0.5 was used. The DEER traces were simulated in the time domain up to 8 µs. For each parameter set we generated ten different traces. To compare the background correction by division (Jeschke et al., 2006) with the kernel inclusion approach as described in (Fábregas Ibáñez and Jeschke, 2020) we analysed all simulated DEER traces with both methods. We did not fit the background but used the true background function. The regularisation parameter was chosen according to the generalised cross-validation method. The quality of the resulting distance distributions p was estimated by the Euclidian distance D from the true distance p_0:

$$D(p, p_0) = \|p - p_0\|_2 \tag{1}$$

The MNR of the form factor F was calculated as described in the main text up to a limit of 7 µs according to equation (13) of the main text.

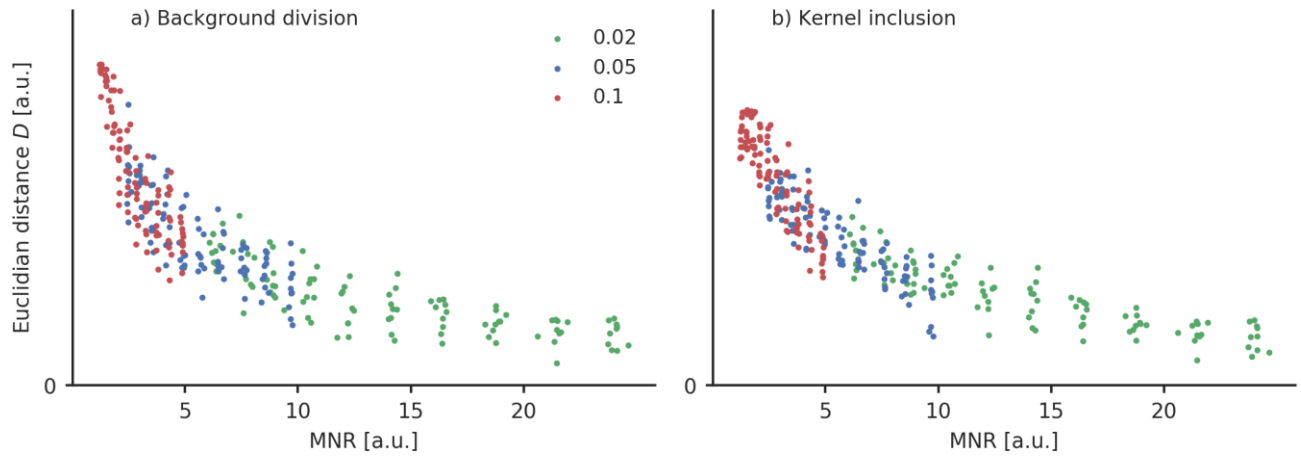

Figure S2: The Euclidian distance D of the real and calculated distance distribution as defined in equation (1) is plotted as a function of the MNR. Each dot represents a simulated DEER trace with either low (σ_0 = 0.02, green), medium (σ_0 = 0.05, blue) and high (σ_0 = 0.1, red) noise. The background correction was performed by (a) dividing the DEER trace by the background and (b) including the background in the kernel.

In Fig. S2, the quality of the determined distance distribution was plotted as a function of the determined MNR for both a background correction by division (Fig. S2a) and a kernel inclusion approach (Fig. S2b). For each noise level the MNR only depends on the density of the background as all other parameters are kept constant and only the background density is varied. So a lower MNR corresponds to a higher background density rate and vice versa. For the low noise level (σ_0 = 0.02), the quality of the determined distance distributions only varies a little for different background density rates. For medium (σ_0 = 0.05) and high (σ_0 = 0.1) noise levels, however, the dependency of the quality of the determined distance distribution decreases significantly with a decreasing MNR. If the MNR is only evaluated up to an early point of the form factor, the information of the background decay rate is lost in this case and is not properly included in the MNR as the MNR would then depend nearly exclusively on the given noise level.

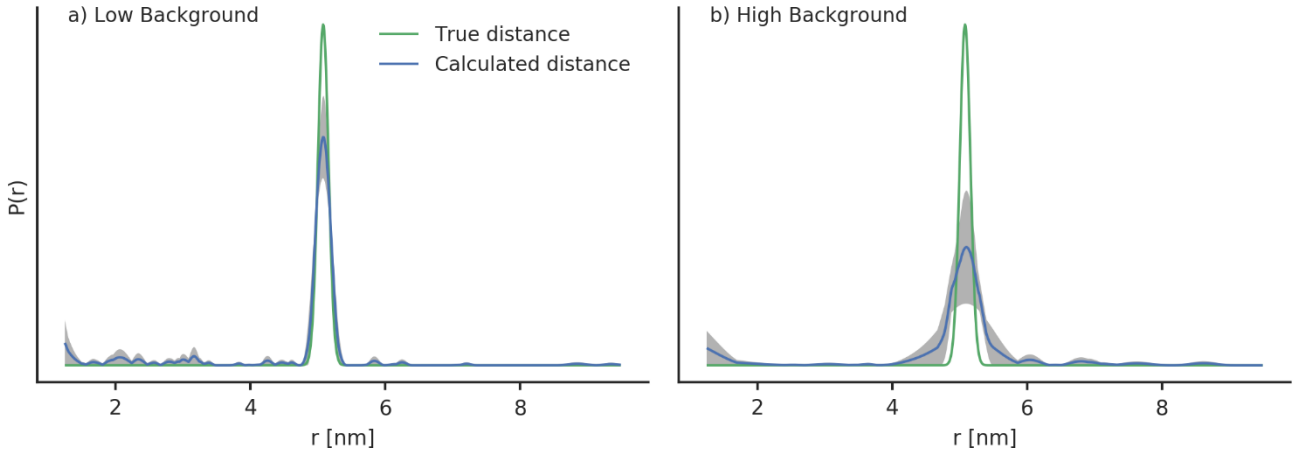

Figure S3: An exemplary distance distribution obtained for a medium noise level (σ_0 = 0.02) with (a) a low background density (k = 0.01 MHz) and (b) a high background density (k = 0.3 MHz). The grey area shows the area that is covered by the calculated distance distribution for ten exemplary DEER traces. The mean of the shaded area is drawn in blue and the true distance is drawn in green.

A closer inspection reveals that whereas the obtained distance distributions for high background densities reproduce the mean of the distance distribution correctly, they overestimate the width of the distribution and the distance appears to be broader as it is (see Fig. S3 for an exemplary data set). Depending on the information that shall be obtained by the DEER measurements, the mean of the distance distribution might suffice. However, if high resolution distance distributions shall be obtained, it seems to be important to optimise the MNR up to the limit which is given by equation (13) of the main text. The comparison of both background correction methods shows that the kernel inclusion gives better results particularly for a high noise and a high background decay. It should therefore be considered as the superior method. However, the correlation between the quality of the determined distance distribution and the MNR is still valid. This is why, we consider the MNR as a proper function of merit, even if the kernel inclusion approach is used.

For a more comprehensive study, the effect of the MNR on the quality of the obtained distance distribution could also be tested for distance distributions with different distance ranges and widths. Such a detailed study was, however, beyond the scope of the this manuscript.

[2] Discuss in more detail whether and how the findings in this work are applicable to other samples (different distance distributions, different concentrations) and spectrometers (different resonator profiles, different Tx fidelity). From the current manuscript, itis unclear whether the findings are generalizable. This is important, since it appears to be the purpose of the manuscript to make some general statements about experimental settings in DEER.

We have added a section in the main text to discuss the effect of different resonator profiles

Depending on the resonator and the microwave amplifier, different B_1 field strengths are available on different spectrometers. However, as the inversion efficiency of broadband shaped pulses is less dependent on the B_1 field strength as is the case for rectangular and Gaussian pulses, who always require a proper adjustment of the pulse length, we assume the findings here to be rather generalisable. In order to discuss this more quantitatively we simulated inversion profiles of the best performing pulses from Table 3 for B_1 field strengths.

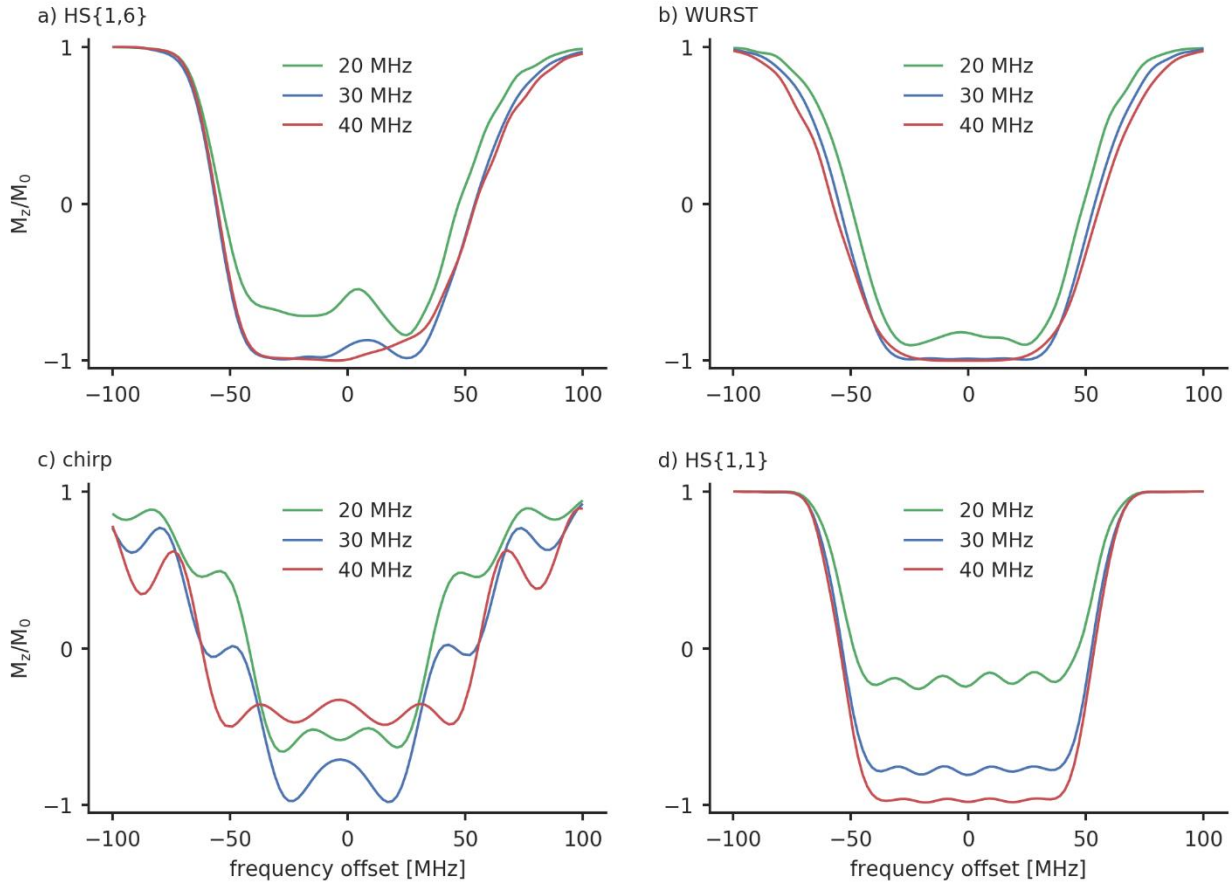

Figure 6: The inversion profiles of the best performing (a) HS{1,6}, (b) WURST, (c) chirp and (d) HS{1,1} pulses with the parameters from Table 3. They were simulated with a B_1 field strength of 20 MHZ (green), 30 MHz (blue) and 40 MHz (red). These field strengths correspond to a π-pulse lengths of 25.0 ns, 16.7 ns (which approximately correspond our setup) and 12.5 ns. The B_1 field here is depicted as the Rabi frequency.

We compare the pulse profiles with B_1 = 30 MHz, which corresponds our setup, with the cases where a lower (B_1 = 20 MHz) or higher (B_1 = 40 MHz) B_1 field strengths arereached. Figure 6 shows how the different pulses behave, when different B_1

field strengths are used. The WURST pulse (Fig. 6b) shows the least variation for different B_1 field strengths. As expected the inversion efficiency drops a little bit for B_1 = 20 MHz. But this drop seems to be rather insignificant and good modulation depths can still be expected. The decrease in inversion efficiency is a bit more significant for the HS{1,6} pulse so that a small reduction in the modulation depth is possible here. Both pulse profiles do not show significant changes when a higher B_1 field strength is used. The HS{1,1} pulse has a massive drop in inversion efficiency when going to lower B_1 field strengths. This comes not as a surprise as the inversion efficiency is already incomplete at B_1 = 30 MHz. Here, it might be advantageous to reduce the β parameter of the HS{1,1} pulse. As it has been stated earlier this will increase the inversion efficiency. For a higher B_1 field strength of B_1 = 40 MHz the inversion efficiency of this HS{1,1} will increase. Therefore, a higher modulation depth comparable to the HS{1,1} pulse is expected. As this will also increase the background decay, a higher MNR is not guaranteed. The chirp pulse also shows a rather strong decrease in the inversion efficiency for a B_1 = 20 MHz. However, the inversion efficiency also decreased for a higher B_1 field strength of B_1 = 40 MHz. This rather unexpected behaviour is probably caused by an insufficient smoothing of the edges of the chirp pulse. With higher B_1 field strength the initial effective magnetic field vector in the accelerated frame becomes less aligned with the z-axis. Therefore, smoothing becomes more important. In Fig. S10, we compared the inversion profiles of 36 ns and 100 ns chirp pulses with and without quarter sine smoothing. When quarter sine smoothing is applied, chirp pulses can with a length of 36 ns indeed reach a high inversion efficiency with B_1 = 40 MHz. (Fig. S10b). As the width of the inversion profile of this chirp pulse drops significantly for smaller B_1 field strengths, it is only advisable to implement a quarter sine smoothing with chirp pulses of a length of 36 ns when enough microwave power is available. The situation looks different for chirp pulses with a pulse length of 100 ns. Here, the inversion profile looks very similar for all tested B_1 field strengths. Particularly for smaller B_1 field strengths we expect 100 ns chirp pulses to outperform chirp pulses with a length of 36 ns.

Another crucial parameter for DEER measurements that can vary from setup to setup is the width of the resonator profile. Here, we have a FWHM of approximately 200 MHz. Larger widths do not seem to be necessary because they would exceed the width of the spectrum of the nitroxide. If only a smaller width is available, the offset between pump and observer pulses might need to be reduced. This would increase the overlap between the observer and pump pulses. This problem could be overcome by either using longer pump pulses or reducing the frequency width of the broadband shaped pulses. As a narrower resonator profile is also necessarily steeper, it might also be necessary to perform a resonator bandwidth compensation as suggested by (Doll et al., 2013). Performing a resonator bandwidth compensation with our setup does not give a significant advantage in the η_{2p} value (see S15). This is probably due to the rather flat resonator profile in the region with maximum sensitivity where the pump pulse is applied.

We have also added the following two sections to discuss different distances ranges and concentrations:

For a concentration of 80 µM, a high MNR improvement can be achieved if the maximum distance of interest is below 4 nm with pulse that achieves a high modulation depth. This would correspond to the HS{1,6} and WURST pulse in this case. If longer distances up to 5 nm shall be detected, it seems to be advantageous to use pulses that might not give the highest modulation depth in order to reduce the background decay. An extrapolation for higher truncation times shows that if even longer distances are of interest, broadband shaped pulses will not give a better MNR compared to rectangular pulses. Here, it is necessary to reduce the background decay by using lower concentrations.

When the MNR shall be increased by using broadband shaped pulses to detect long distances > 5 nm, lower concentrations are preferable as they reduce the enhancement of the background decay. Here, switching to a concentration of 30 µM of the doubly labelled ligand was enough the significantly reduce the influence of the background. In S19 we performed analytical calculations to estimate the potential MNR increase that can be achieved by switching to broadband shaped pulses for different concentrations and distance ranges. For maximum distances below 4 nm an increase of the MNR can be expected for all concentrations up to approximately 100 µM. The situation is different if distances over 6 nm shall be detected. A significant gain can only be expected for smaller concentrations in the range between 10-30 µM. For higher concentrations the MNR gain drops quickly. For higher concentrations in the range of 80 µM a MNR decrease has to be expected in this distance regime. This is discussed in more detail in S21.

[3] - Eq.(3): Specify that the time axis is defined such that t=0 at the center of the pulse.- Eq.(11): (k*|t|)ˆ(d/3) instead of k*tˆ(d/3) - Eq.(12): A factor of 2 might be missing. -8.13: "i.e. a chirp pulse" - 12.18: Here, it is not clear how the numbers for the minimum detectable distance limit are obtained. - Kupce needs a grave accent on the c. Bohlen needs an umlaut on the o. - SI Eq.(2): t_truncation instead of tau_2

We thank the referee for these remarks and corrected and clarified these points.